EXPERIENCE THE FREEDOM OF GOING MOBILE.

A career in mobile surgery offers you...

JOB FREEDOM

MOVES is a national mobile surgery company that emphasizes **quality of life** as our number one value. Our surgeons manage their own schedules with **no emergency or on-call** requirement. MOVES is hiring surgeons in markets across the country.

REWARDING COMPENSATION

All MOVES™ surgeons receive a competitive base salary and **industry-leading production rates.** Our benefits package includes a new company vehicle, healthcare, flexible time off, and retirement. Tenured employees are eligible to participate in our **profit-sharing** program and employee liquidity pool.

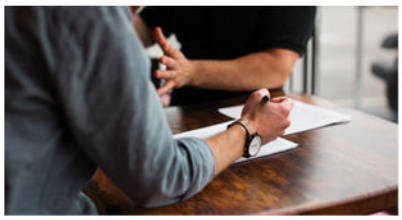

WORLD-CLASS SUPPORT

MOVES™ makes starting a mobile surgery practice easy. Our dedicated support tream walks you through everything from choosing and ordering equipment to marketing and invoicing. We make start-up simple so you can **focus on your patients.**

MOVES™

Now hiring small animal surgeons nationwide!

Click to apply now or visit us at www.VetMoves.com for more info.

APPLY NOW

Learn More and Apply at VetMoves.com

Received: 30 October 2017 | Revised: 11 October 2018 | Accepted: 6 November 2018

DOI: 10.1111/vsu.13373

ORIGINAL ARTICLE - RESEARCH

WILEY

Preliminary evaluation of an osteochondral autograft, a prosthetic implant, and a biphasic absorbable implant for osteochondral reconstruction in a sheep model

Mélanie Olive DVM[1] | Cécile Boyer PhD[2] | Julie Lesoeur MS[2] | Chantal Thorin PhD[3] | Pierre Weiss DDS, PhD[2] | Marion Fusellier DVM, PhD[1,2] | Olivier Gauthier DVM, PhD[1,2]

[1]Department of Small Animal Surgery, Oniris Nantes-Atlantic College of Veterinary Medicine Food Science and Engineering, Nantes, France

[2]University of Nantes, INSERM UMR 1229, RMeS, Nantes, France

[3]Department of Management and Statistics, Oniris Nantes-Atlantic College of Veterinary Medicine Food Science and Engineering, Nantes, France

Correspondence
Olivier Gauthier, Department of Small Animal Surgery, ONIRIS Nantes-Atlantic College of Veterinary Medicine, Food Science and Engineering, Site de la Chantrerie, CS 40706, 44307 Nantes Cedex 3, France.
Email: olivier.gauthier@oniris-nantes.fr

Abstract

Objective: To determine the ability of three implants to enhance the healing of osteochondral defects: (1) a biphasic construct composed of calcium phosphate (CaP) and chitosan/cellulosic polymer, (2) a titanium-polyurethane implant, and (3) an osteochondral autograft.

Study design: Experimental study.

Animals: Ten adult female sheep.

Methods: In five sheep, an 8-mm diameter osteochondral defect was created on the medial femoral condyle of a stifle and filled with a synthetic titanium-polyurethane implant. In five sheep, a similar defect was filled with an osteochondral autograft, and the donor site was filled with a biphasic construct combining CaP granules and a chitosan/cellulosic polymer. Sheep were monitored daily for lameness. Stifle radiographs and MRI were evaluated at 20 weeks, prior to animals being humanely killed. Surgical sites were evaluated with histology, microcomputed tomography, and scanning electron microscopy.

Results: Clinical outcomes were satisfactory regardless of the tested biomaterials. All implants appeared in place on imaging studies. Osteointegration of prosthetic implants varied between sites, with limited ingrowth of new bone into the titanium structure. Autografts and biphasic constructs were consistently well integrated in subchondral bone. All autografts except one contained a cartilage surface, and all biphasic constructs except one partially restored hyaline cartilage surface.

This study was presented at the 26th European College of Veterinary Surgeons annual scientific meeting; July 13-15, 2017; Edinburgh, Scotland.

Conclusion: Biphasic constructs supported hyaline cartilage and subchondral bone regeneration, although restoration of the articular cartilage was incomplete.

Clinical impact: Biphasic constructs may provide an alternative treatment for osteochondral defects, offering a less invasive approach compared with autologous grafts and eliminating the requirement for a prosthetic implant.

1 | INTRODUCTION

Osteochondral reconstruction seeks to restore the articular cartilage surface and associated subchondral bone. In veterinary surgery, the most common treatment option for osteochondrosis (OC) associated lesions relies on bone marrow stimulation, through curettage, abrasive chondroplasty, microfracture and microdrilling. These techniques were introduced decades ago and typically result in the formation of fibrocartilage and associated osteoarthritis.[1] Osteochondral bone grafting is well documented as an alternative to treat OC and OC dissecans lesions.[2-5] This approach remains invasive and may be limited by donor site availability and suitability as well as induced morbidity.[6,7] Nonabsorbable prosthetic implants have recently been proposed to lead to satisfactory clinical outcomes when used as alternatives for osteochondral reconstruction in dogs and horses.[8-11] Cell-based strategies such as autologous-chondrocytes implantation with or without an associated matrix have become widely used in man in the past two decades.[12,13] However, the long-term benefits of these techniques compared with bone marrow stimulation have not been established.[14-16]

The development of acellular polymers may provide an attractive alternative to overcome the cost and complexity of cell-based approaches.[17] Chitosan is one of the most widely investigated polymers for regenerative medicine, in particular for cartilage regeneration because it displays structural properties that are similar to natural glycosaminoglycans.[18-20] Chitosan promotes the expression of cartilage matrix compounds and reduces production of inflammatory and catabolic mediators by chondrocytes.[21] A chitosan gel has been combined with microfracture to stabilize the blood clot and factors obtained from bone marrow stimulation, resulting in superior cartilage repair compared with microfracture alone up to 5 years postoperatively.[22] Hydroxypropylmethylcellulose (HPMC) provides a suitable environment for autologous stroma cells and chondrocytes[23] and induced cartilage formation with a hyaline-like organization in a rabbit cartilage defect model.[24] Chitosan and HPMC are polysaccharides that can be combined and chemically silanized to provide self-hardening properties in vivo.[17,25]

Synthetic absorbable biphasic constructs have been proposed as osteochondral substitutes,[26,27] typically consisting of an upper polymeric surface designed to favor chondrogenesis and a deeper component composed of ceramic or collagen to promote integration into the subchondral bone. Such scaffolds have yielded divergent results in clinical studies of human patients and warrant further investigation.[28-30] Calcium phosphate (CaP) bone substitutes such as hydroxyapatite, tricalcium phosphate, and mixtures of these compounds are widely used as bone substitutes.[31] Although they have been proposed as a subchondral base for biphasic constructs combined with HPMC or chitosan,[32] none of the proposed biphasic constructs combined CaP granules and an injectable self-setting polysaccharide polymer.

The objective of this experimental study was to compare three strategies for osteochondral reconstruction in an ovine model of femoral OC lesions: (1) a reconstructive approach with an autologous osteochondral graft, (2) a prosthetic approach with a titanium-based osteochondral implant, and (3) a matrix-induced osteochondral regenerative approach with a biphasic absorbable construct to fill donor sites of osteochondral transplants. Our hypothesis was that biphasic constructs combining a CaP subchondral base and a polymeric HPMC-chitosan superficial layer would allow subchondral bone and hyaline cartilage regeneration in experimental osteochondral defects.

2 | MATERIALS AND METHODS

2.1 | Experimental design

This study was conducted with 10 adult female sheep (65 ± 5 kg) after approval by both national CEEA N°6 Pays de la Loire and Oniris local ethical and animal welfare committees (No. 2012.120). The animals were checked preoperatively for the absence of bone or joint disease on the relevant limbs, with assessment by clinical examination and radiographs of stifle joints.

2.2 | Surgical model

General anesthesia was induced by IV injection of diazepam (0.2 mg/kg), ketamine (5 mg/kg), and propofol (4-6 mg/kg, to effect) associated with epidural anesthesia (bupivacaine, 1 mg/kg) and maintained with isoflurane in pure oxygen. With the animal in dorsal recumbency, a medial arthrotomy of the stifle joint with section of the distal attachments of the vastus medialis muscle was performed on the left hindlimb of each animal. After lateral luxation of the patella, a calibrated 8-mm-diameter osteochondral defect was created in the center of the medial femoral condyle mimicking an OC lesion. In five animals, the defect was created with a calibrated reamer of appropriate diameter and depth. The defect was filled with an 8-mm prosthetic titanium-polycarbonate/urethane implant (SynACART; Arthrex VetSystems, Ft Meyers, Florida) according to the surgical technique recommended by the manufacturer. SynACART implants are composed of a 4-mm-thick subchondral titanium base and an approximately 3.5-mm-thick polycarbonate urethane superficial layer. In five other animals, an 8-mm-diameter and 10- to 15-mm-deep femoral defect was created in the center of the medial femoral condyle and filled with an autologous osteochondral transplant (OATS technique; Arthrex VetSystems). The transplant was harvested from the proximal axial inner aspect of the femoral trochlea and transferred into the receiver site. Depth of the defects was checked with a dedicated graduated periodontal probe.

Donor cores were 2 to 3 mm longer than the depth of receiver sites and adjusted to the final depth by using a scalpel blade to ensure good press fit impaction. The donor site was filled with CaP ceramic granules 0.5 to 1 mm in diameter (BCP; Graftys, Aix-en-Provence, France) and an injectable self-setting silanized chitosan/HPMC copolymer (2%/2% weight ratio, respectively), providing a substitute for the subchondral bone and the articular cartilage surface, respectively (Figure 1). Calcium phosphate granules filled the base of the defect up to 2 mm from the top of the defect. The polymer was prepared perioperatively and then injected above the granules to provide an approximately 2-mm-thick superficial layer. The patella was returned to its position, and the stifle joint was mobilized several times in flexion and extension. Implant placement was checked before closure of the routine closure of the muscular, capsular, subcutaneous and cutaneous tissues with monofilament absorbable sutures.

Immediately after surgery, the animals were confined to individual runs for 5 days and then allowed to move freely in collective runs. Administration of prophylactic antibiotics was limited to 30 mg/kg IV cephalexin at the time of induction. Postoperative analgesia consisted of oral meloxicam (0.1 mg/kg) administration for 5 days, associated with fentanyl delivered through a transdermal patch (50 μg/h).

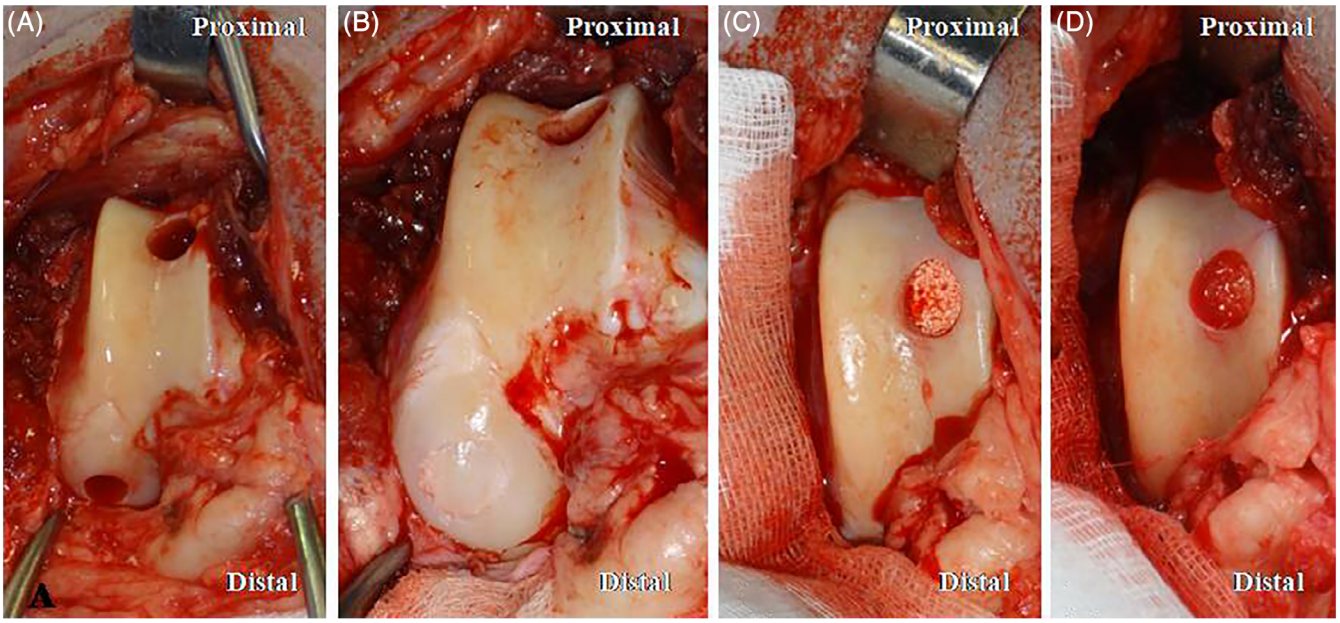

FIGURE 1 Intraoperative views of autogenous osteochondral reconstruction with the OATS system. A, The donor core, 8 mm in diameter, was harvested at the proximal axial aspect of the trochlea. Receiver site was located on the medial femoral condyle mimicking an OC lesion. B, The donor core was transplanted into the receiver site. C, The receiver site was filled with 0.5 to 1 mm CaP granules up to 2 mm from the articular surface. D, The HPMC/chitosan self-setting polymer was injected onto the CaP granules. CaP, calcium phosphate; HPMC, hydroxypropylmethylcellulose; OC, osteochondrosis

2.3 | Postoperative care and follow-up

Animals were inspected twice daily for the first postoperative week and once per day for the rest of the implantation period. Physical and orthopedic examinations were performed every day, with the observer unaware of the treatment group. Postoperative lameness was graded as 0 = no lameness, grade 1 = slight intermittent weight-bearing lameness, grade 2 = slight to moderate persistent weight-bearing lameness, grade 3 = severe persistent weight-bearing lameness, and grade 4 = persistent non–weight-bearing lameness. Twenty weeks after implantation, radiographic and MRI examinations of the stifle were performed with the animals in dorsal recumbency and under general anesthesia. T1 3D Vibe, T1 TSE, and T2 TSE sequences (Magnetom Essenza 1.5T; Siemens, Munich, Germany) were used for MRI examination. Animals were then humanely killed with an IV overdose of pentobarbital, and the distal femoral ends were immediately dissected for macroscopic evaluation.

2.4 | Histological analysis

The distal femoral ends were cut into blocks preserving 5 mm of intact surrounding tissues around the different implantation sites and stored at −20°C. Blocks were placed during 2 hours in water at room temperature before microcomputed tomography (μCT) imaging could be performed (Skyscan 1272; Bruker, Belgium). Scanning analysis was performed at 22-μm isotropic resolution with the x-ray tube operated at 80 kV and 125 μA. Image analysis was performed in NRECON and CTAn software for image reconstruction and segmentation and CTVox and DataViewer software (Bruker; https://www.bruker.com/products/microtomography/micro-ct-software/3dsuite.html) for three-dimensional visualization of the scanned areas. Specimens were then fixed in 4% paraformaldehyde solution, placed overnight in a 2% phosphotungstic acid (PTA) solution, progressively dehydrated in graded ethanol, and finally embedded in an acrylic resin (Technovit GMA; Kulzer, Hanau, Germany). All specimens were cut into halves according to the diameter and parallel to the long axis of the defect with a circular diamond saw (SP1600; Leica, Wetzlar, Germany), providing two surfaces that were polished (Metasery 2000, Buehler, Esslingen, Germany) and sputtered with gold-palladium (Desk III vacuum; Denton, Moorestown, New Jersey) before scanning electron microscopy (SEM) analysis was performed by using backscattered electron imaging (LEO 1450VP; Carl Zeiss, Oberkochen, Germany).

Light microscopy histology was performed on 5-μm-thick sections (microtome Polycut SM2500; Leica, Nanterre, France) stained with hematoxylin and eosin, Goldner's trichrome, Movat's pentachrome, and collagen type 2 immunohistochemical stains for both autologous transplants and biphasic implants,. Prosthetic implants provided 50-μm-thick sections that were stained with methylene blue and basic fuchsin.

Osteointegration of the different types of implants was investigated, including (1) the interface between the porous titanium implant and the host bone as well as bone ingrowth into the porous titanium structure, (2) the subchondral bone restoration after autologous transplantation or CaP granules bone filling of the donor site, and (3) the characteristics of the prosthetic, autologous or newly formed cartilaginous surface.

Based on two-dimensional images from SEM, image analysis (ImageJ2 software; Fiji, Tokyo, Japan) allowed measurement of (1) the amount of newly formed bone into the porous titanium structure of prosthetic implants (bone surface / total surface), (2) the amount of newly formed bone into donor sites filled with the CaP granules of biphasic constructs, and (3) the amount of transplant subchondral bone in receiver sites. Cartilage surface integration or regeneration was investigated qualitatively on histological μCT and stained sections.

2.5 | Statistical analysis

The quantity of bone (bone surface / total surface) was compared with the three conditions detailed above, according to the measurements obtained from image analysis. To take into account of the repeated measurement design, the respective percentages of bone tissue were adjusted to experimental conditions by using a linear mixed effects model with individual as random effect. Model validity conditions were checked, and pairwise comparisons between the different conditions were performed by using Tukey constrasts in the fitted model. Statistical analysis was performed with nlme and multcomp library in R (R Foundation for Statistical Computing, Vienna, Austria. http://www.R-project.org/.). $P < .05$ was considered significant.

3 | RESULTS

3.1 | Clinical and macroscopic examinations

All implants and transplants were placed successfully, and all animals recovered from surgery. Postoperative lameness improved from grade 3 to 4 to grade 1 to 2 after two weeks and continued improving throughout the

implantation period. No infection or swelling was observed from the surgical site, and no complication was recorded throughout the implantation period, regardless of the nature of the implant. Twenty weeks after surgery, residual lameness was still observed in two animals with prosthetic implants (grade 1 and 2) and in two animals with autologous transplants (grade 2).

After animals had been humanely killed, all implants appeared in place on macroscopic examination (Figure 2), without gross evidence of instability or damage to their synthetic articular surface. Autologous transplants were also all in place, but one exhibited major cartilaginous surface damage resembling an OC lesion. One transplant seemed subsided by less than 1 mm, and the receiver site edges appeared covered by white and smooth newly formed tissue. The surface of the donor site defects was covered with a white, opaque, regular and smooth tissue, but an uncovered area remained in the central part of most of the defects except one that appeared completely covered.

3.2 | Radiographic examination

All prosthetic implants and biphasic constructs appeared in place according to radiographs. Two prosthetic implants were surrounded with a radiolucent line consistent with residual instability and poor osteointegration. Patella osteophytosis and effusion were detected on four joints, regardless of the implants in place. No lesions into the subchondral bone were observed around the different implantation sites. Receiver sites on the medial femoral condyle were still slightly visible on mediolateral radiographic views. Donor sites could be easily identified due to the radiopacity of the CaP granules (Figure 3).

3.3 | Magnetic resonance imaging examination

Residual synovitis was observed in joints with autologous transplants. One extensive subchondral bone lesion

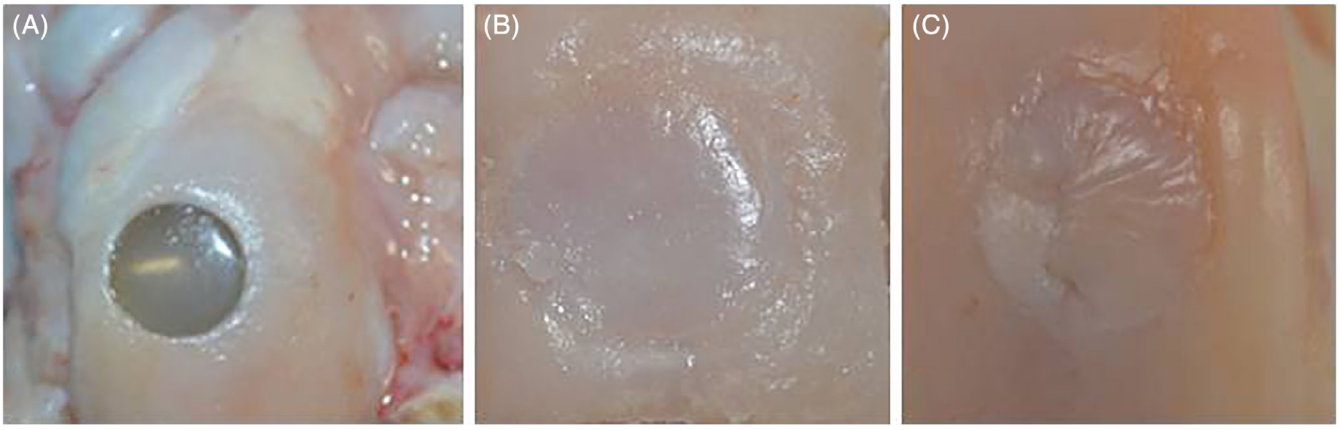

FIGURE 2 Representative macroscopic appearance of a prosthetic SynACART implant (A), a receiver site filled with the osteochondral autograft (B), and a donor site filled with the biphasic construct (C)

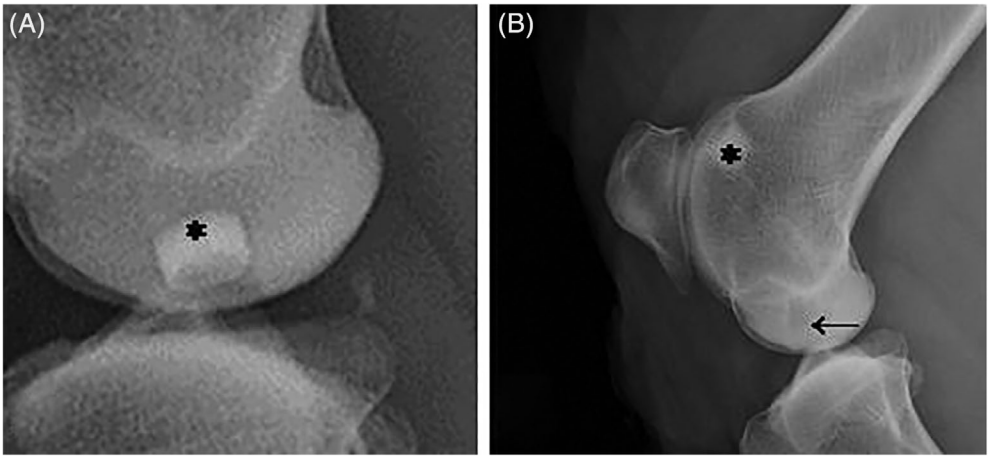

FIGURE 3 Mediolateral radiographic views of a prosthetic SynACART implant whose titanium subchondral base is visible (*; A), a receiver site filled with the osteochondral autograft (→; B), and the corresponding donor site filled with the biphasic construct (*; B)

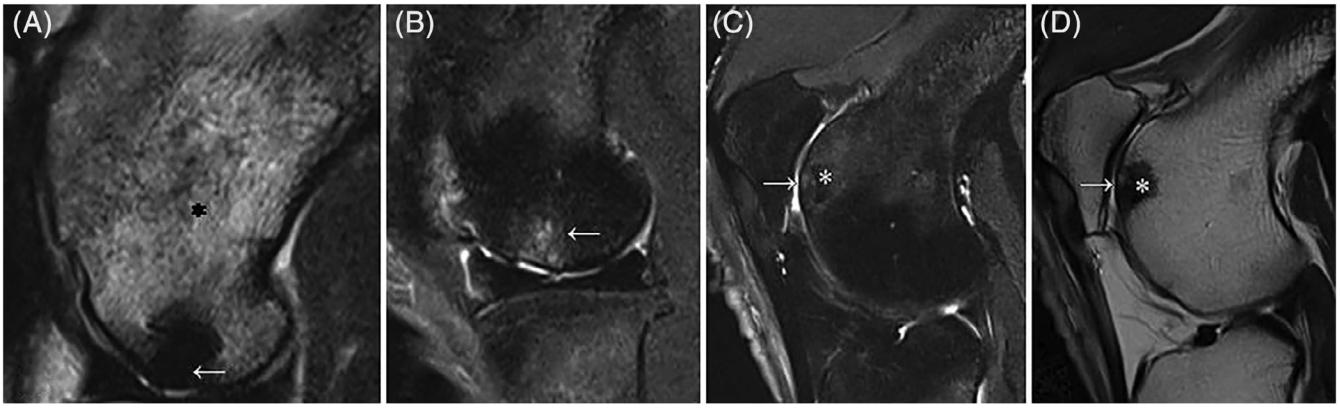

FIGURE 4 MRI views in T2 TSE (A-C) and T1 TSE (D) sequences. A, The prosthetic SynACART implant (←) is visible in all contrasts associated with significant edema in the epiphysis trabecular bone (*). B, Receiver site filled with the osteochondral autograft (←) with a slight subsidence of the transplant and some cavities in the transplant subchondral bone. C,D, The corresponding donor site filled with the biphasic construct (*) is visible in T2 TSE (C) and T1 TSE (D) weighted images. The two images allow the assessment of the congruity of the newly formed cartilage surface deemed satisfactory (→). Remaining calcium phosphate granules are still visible

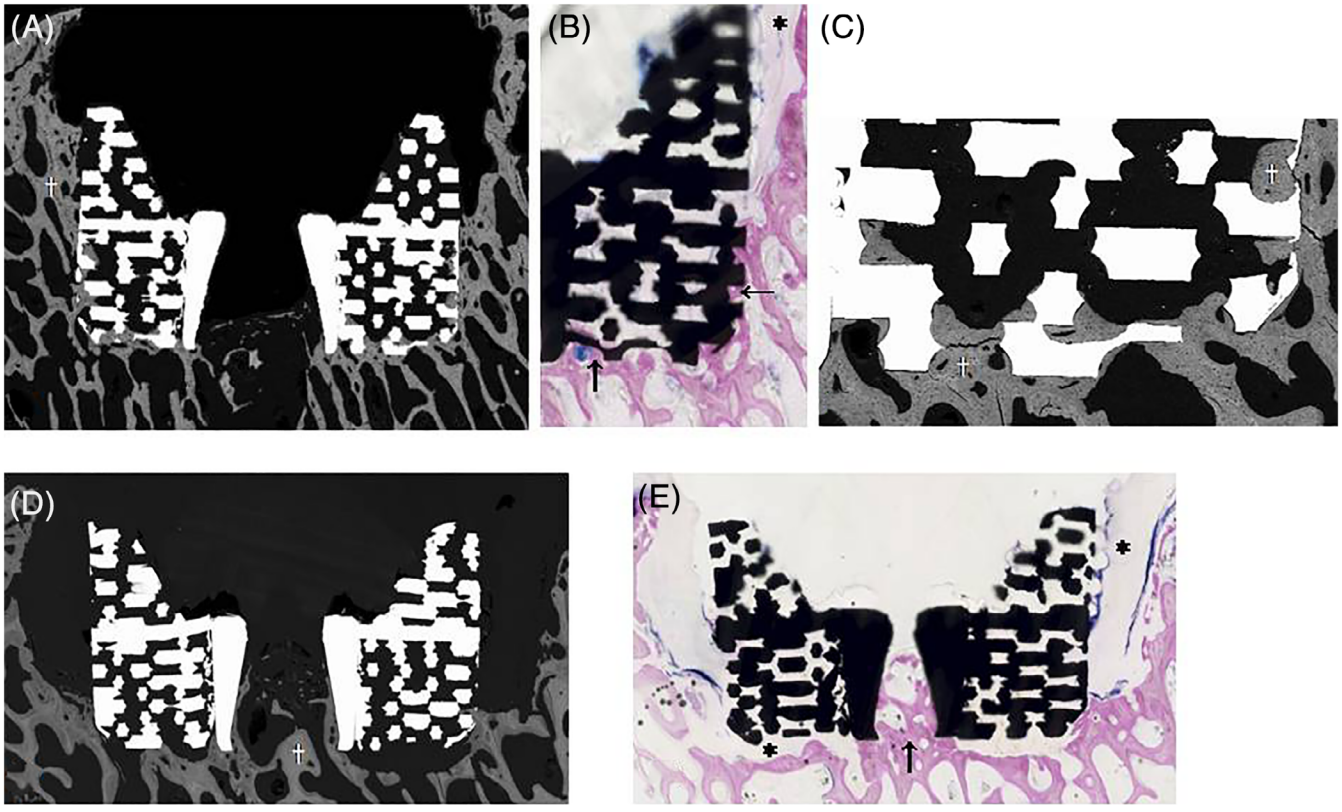

FIGURE 5 Histological images of prosthetic titanium-based implants. Sections were parallel to the long axis of the defect. A, SEM image. Titanium appears in light white. Bone tissue appears in gray (†). New bone formation is visible in close contact with the implant surface and inside the porous structure. The polycarbonate urethane superficial part of the implant is not visible. B, Methylene blue-fuchsin stain. Details of new bone apposition onto and into the titanium structure (→). Fibrous connective tissue is present on the upper part of the implant (*). C, SEM image. Details of the new bone formation (†) into the pores of the titanium structure, in close contact with the implant surface. D, SEM image of another implant. New bone apposition (†) is limited to the deep part of the implant. E, Methylene blue-fuchsin stain. New bone ingrowth is present only in the central part of the implant (→), and fibrous connective tissue is present both on the upper and deep parts of the implant (*). SEM, scanning electron microscopy

TABLE 1 Percentage of bone[a] determined by image analysis on SEM images into prosthetic implants, biphasic constructs, and autologous transplants

New bone formation into prosthetic implants, %	New bone formation in biphasic constructs, %	Bone content in autologous transplants, %
5.38 ± 1.64%	28.63 ± 4.01%	40.03 ± 9.27

Note: Values are mean ± SD. Percentage of bone tissue differed between treatments with $P < .001$, except the difference between autologous transplants and biphasic constructs with $P = .0175$.
Abbreviation: SEM, scanning electron microscopy.
[a]Bone surface / total surface.

(edema, necrosis) was observed associated with one prosthetic implant, and a subchondral tibial plateau edema was associated with another. Autologous transplants exhibited a preserved cartilage surface in all but one transplant. The original profile of the articular surface appeared at least partially restored in all donor sites and in continuity with the surrounding articular surface, with one site exhibiting completely new cartilage surface (Figure 4).

3.4 | Microcomputed tomography and SEM examinations

Microcomputed tomography did not provide relevant images of SynACART implants due to artefacts created

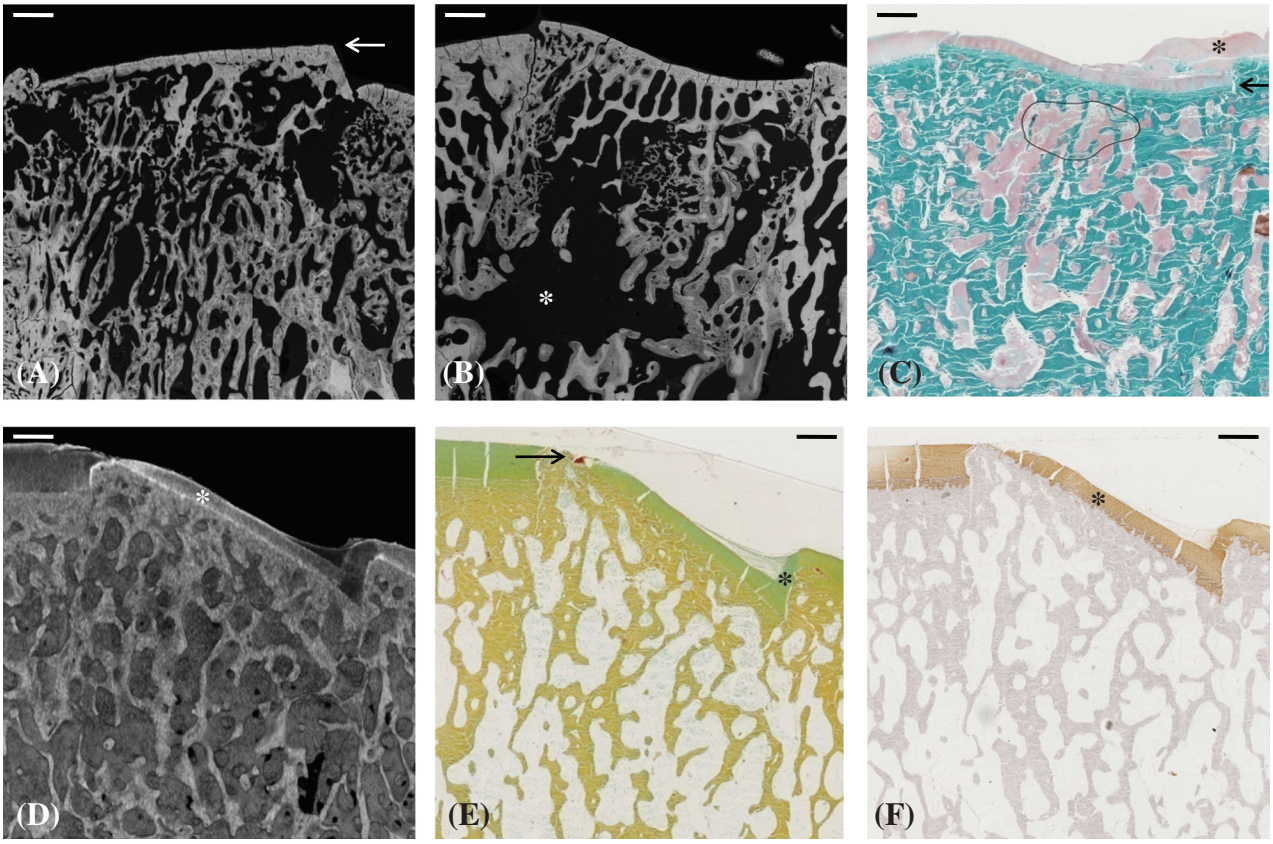

FIGURE 6 Histological images of receiver sites after autologous osteochondral transplantation. Sections were parallel to the long axis of the defect. A, SEM image. Bone tissue appears in gray. The donor core subchondral bone appears well integrated into the host bone. A slight offset of the transplant (←) is visible at the right junction with the host bone. B, SEM image confirming the viability and osteointegration of the transplant where some void spaces are visible (*). The surface of the donor core appears concave as the receiver site displays a convex curvature. C, Goldner's trichrome stain image of the previous transplant. Bone healing of the transplant appears very satisfactory. Despite a slight subsidence at the right junction (←), newly formed cartilage has covered this part of the transplant surface (*). D, μCT image. Thanks to PTA treatment, the superficial cartilage layer is visible (*), with a slight difference in cartilage thickness between the transplant and the receiver site. E, Movat's pentachrome stain of the previous transplant illustrating similar mineralization of the transplant subchondral bone and receiver. Cartilage continuity is observed despite a slight subsidence on the right side of the transplant (*), whereas cartilage continuity remains incomplete at the left junction (→). F, Collagen type 2 immunohistochemical positive stain (*) into the cartilage surface of the transplant. Scale bar = 1 mm. μCT, microcomputed tomography; PTA, phosphotungstic acid; SEM, scanning electron microscopy

by their metallic structure, but SEM allowed precise description and quantification of new bone formation. Osteointegration varied between prosthetic implants (Figure 5). Despite gross stability, no evidence of new bone formation was found at one implantation site. New bone formation was very limited in two sites, mainly located onto the implant and inside the porous titanium structure. In the last two implants, bone ingrowth and new bone apposition onto the implants were pronounced, especially in the deep subchondral part of the implants. The amount of newly formed bone into the porous titanium structure represented only 5.38% ± 1.64% of the implant porous surface and was lower ($P < .001$) than in all other locations (Table 1).

Subchondral bone healing was consistent at sites treated with autologous transplants. The trabecular structure of the transplant was preserved and osteointegrated in all cases (Figure 6). The bone content of autologous transplants (bone surface/total surface) represented 40.03% ± 9.27% of the defect area (Figure 7).

All biphasic constructs exhibited complete incorporation of the CaP granules into a new bone trabecular network. New bone formation was easily identified between the CaP granules (Figure 8). The amount of new bone formation into the donor sites represented 28.63% ± 4.01% of the defect area (Table 1) and was lower than the bone content in autografts ($P = .0175$).

Treatment of specimens with PTA allowed identification of a cartilaginous surface including the preserved surface of transplants (Figure 6) and the newly formed surface in biphasic constructs (Figure 8). The cartilaginous surface of the transplants appeared preserved with satisfactory continuity with the surrounding host cartilage. No osteophytosis was detected in these junction areas.

3.5 | Histological examination in light microscopy

Inconsistent osteointegration of the prosthetic implants was confirmed by histological examination. No fibrous layer was observed over the polycarbonate urethane articular surface of the implants. Limited new bone ingrowth was observed, mainly at the bottom of the implant site. Fibrous connective tissue was observed around the upper part of the implant preventing further bone colonization (Figure 5).

Reproducible histological features were obtained for autologous transplants and biphasic constructs. Bone healing of the subchondral part of the transplant was obtained in all sites filled with autologous transplants (Figures 6 and 7), with preservation and viability of the hyaline cartilage surface of the transplant (Figure 6). Cartilage thickness varied between transplants and receiver sites (Figure 6-6), and some incongruities were also noticed at the junction areas, together with a few curvature mismatches in the cartilage surface (Figure 6). In donor sites filled with biphasic constructs, complete bone colonization of the intergranular spaces between CaP particles was observed, providing a regenerated subchondral bone basis (Figure 8). Centripetal coverage of the superficial aspect of the donor site by a newly formed hyaline-like cartilage was observed as illustrated by the abundant presence of collagen type 2 on immunohistochemical stains (Figure 8). This coverage remained incomplete in most of the specimens, associated with a slight collapse in subchondral bone filling by the CaP granules in the center of the defects (Figure 8-8). In one specimen, the cartilaginous coverage appeared complete and homogenous over the entire donor site and with thickness similar to the surrounding host cartilage (Figure 8-8).

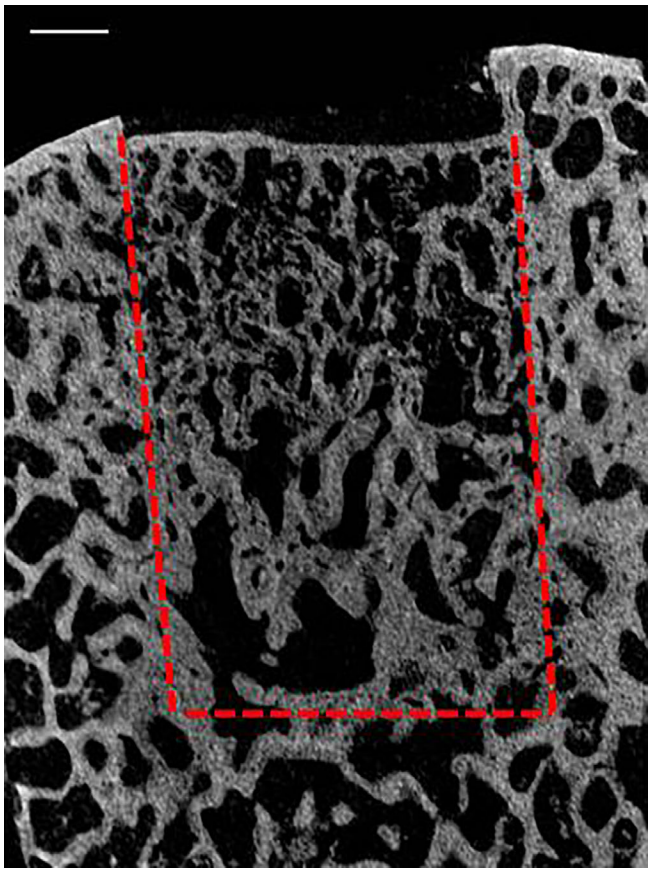

FIGURE 7 Histological two-dimensional μCT image of a receiver site after autologous osteochondral transplantation. Sections were parallel to the long axis of the defect. The dotted line defines the contours of the transplanted core. Osteointegration of the transplant appears very satisfactory. Scale bar = 2 mm. μCT, microcomputed tomography

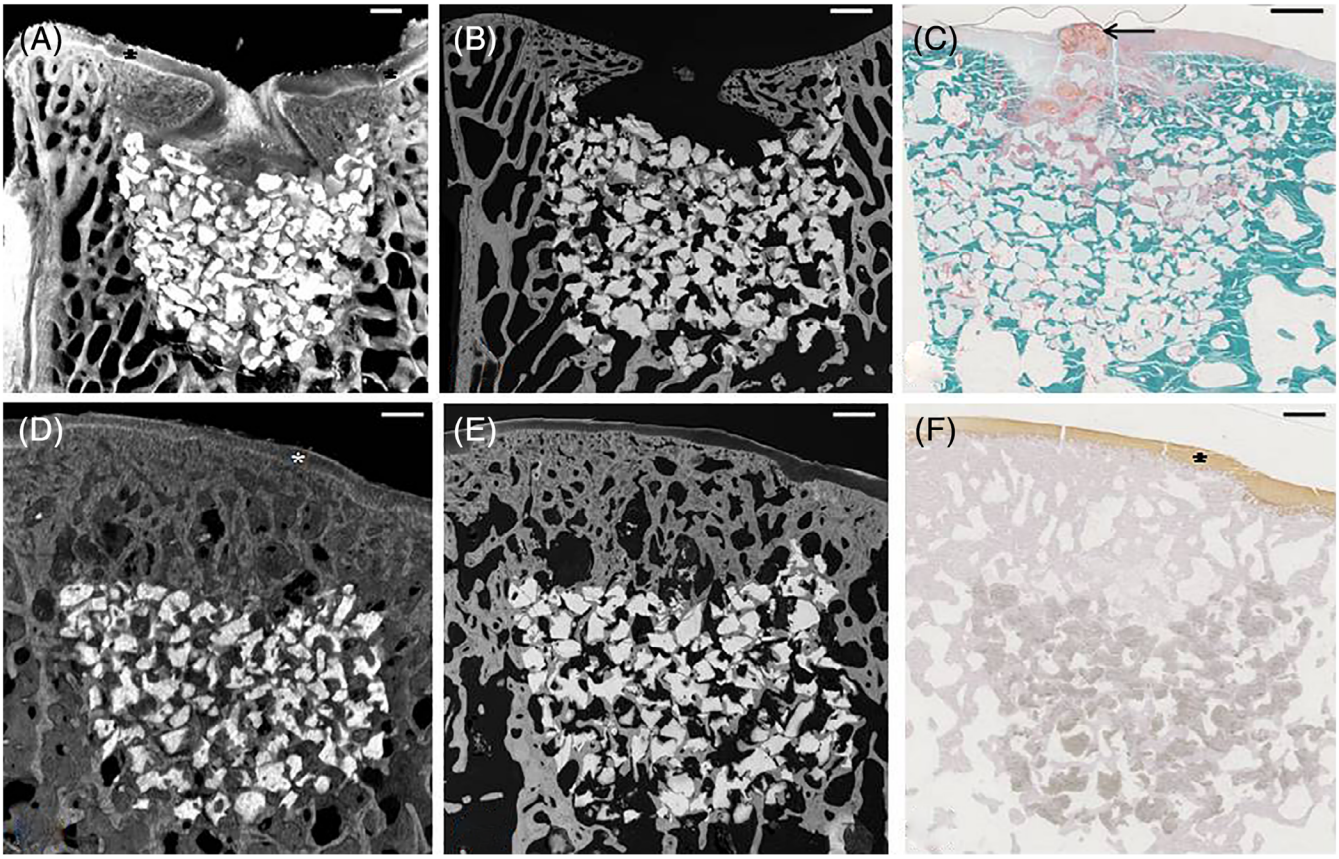

FIGURE 8 Histological images of donor sites filled with the biphasic construct. Sections were parallel to the long axis of the defect. A, μCT image with PTA treatment. Bone tissue appears in gray and CaP granules in bright white. The newly formed cartilage appeared in perfect continuity with the receiver one and with a similar thickness (*). Cartilage coverage remains incomplete in the center of the defect. B, SEM image of the previous donor site. Bone tissue appears in gray, and CaP granules appear in white. A slight collapse of the CaP granules is visible in the center of the defect and subchondral bone restoration is incomplete. C, Goldner's trichrome stain of the previous donor site illustrating the presence of a disorganized connective tissue in the superficial central part of the defect (←). D, μCT image with PTA treatment. Newly formed bone colonized the intergranular spaces joining the CaP granules to each other and restoring the subchondral bone below the new cartilage surface (*) that covered the whole donor site. E, SEM image of the previous donor site illustrating precise details of new bone formation between and above the CaP granules. F, Collagen type 2 immunohistochemical positive stain (*) of the hyaline-like regenerated cartilage surface. CaP, calcium phosphate; μCT, microcomputed tomography; PTA, phosphotungstic acid; SEM, scanning electron microscopy. Scale bar = 1 mm

4 | DISCUSSION

In the present study, implantation of biphasic constructs in donor sites of osteochondral autologous transplants led to consistent integration of CaP granules with adjacent subchondral bone and partial regeneration of the cartilage surface. The newly formed cartilage appeared continuous with the host cartilage and presented a similar thickness. We therefore accept our hypothesis because both subchondral bone and hyaline cartilage regeneration was achieved in all donor sites but one.

Moreover, our study provides a new description of histological features associated with osteochondral reconstruction strategies. Prosthetic implants provided a nonabsorbable permanent cartilage surface that remained intact throughout the study but led to variable osteointegration. New bone ingrowth into the porous titanium structure was limited, although the implant appeared stable according to gross examination. All autologous transplants led to satisfactory healing in the subchondral bone, and all but one retained their hyaline cartilage surface.

Satisfactory bone integration of osteochondral prosthetic implants have recently been reported in several studies of dogs and horses.[8-11] Our findings are consistent with their clinical and radiological results, but histological features should raise concerns regarding long-term osteointegration and stability of nonabsorbable implants.[8,9] In our study, the implant had to be impacted into the defect flush to the receiver articular surface to

provide adequate congruity. As a result, the polycarbonate urethane surface became surrounded with the receiver subchondral bone that may have compromised the initial press fit fixation after weight-bearing was restored. Although such prosthetic implants seem promising,[10,11] they deserve further evaluation and, probably, a refined design, particularly of their porosity and length, to ensure optimal subchondral osteointegration.

Osteochondral grafting requires a compromise between cartilage thickness, curvature of the cartilage surface, and subchondral bone density when determining the most suitable donor site.[33-35] Although preoperative mapping to determine the most suitable donor site was not performed in our study, transplants were harvested from the axial proximal aspect of the trochlea to minimize the risk of surface curvature mismatch between the cartilage from the donor site and the receiver site. Slight differences in cartilage thickness were observed between the transplants and the receiver sites, as was reported in dogs,[34] as well as slight donor core offset or subsidence. Donor cores were of adequate depth in all cases,[2,5] far from the 4-mm anchorage provided by the titanium base of the prosthetic implant. The reliability of autologous osteochondral transplantation to achieve subchondral bone and cartilage reconstruction was confirmed here, but its limitations persist. This invasive technique requires a second surgical site for transplant harvesting and generates morbidity and incongruencies between the transplant and the receiver site. In human patients, donor sites are left unfilled for spontaneous healing or are filled with gelatin or bone wax,[36] potentially leading to osteophytosis and osteoarthritis.[26,37] The morbidity associated with such iatrogenic lesions in animals is mostly considered negligible, although it is poorly documented.[3] Synthetic absorbable biphasic implants may avoid the requirement for autologous transplants and the associated morbidity due to the harvesting procedure. A multilayered collagen 1-hydroxyapatite scaffold provided promising results during early preclinical and human clinical studies, but contradictory long-term results with incomplete cartilage repair and poor subchondral repair.[28,29] A polylactic/polyglycolic copolymer and calcium sulfate combination has been used to fill donor sites and treat primary lesions during OATS [osteochondral autograft transplant system] technique, without any benefit compared with more traditional treatments.[30] An aragonite-hyaluronate osteochondral substitute recently provided promising results for the treatment of articular surface lesions in human patients up to 12 months postoperatively.[38]

Current resurfacing techniques with autologous transplants, prosthetic implants, or other biphasic constructs relies on plugs that must perfectly fit the osteochondral defect geometry to ensure stability and biological integration of the implant. By contrast, the association of CaP granular form and an injectable polymer in our construct allowed the construct to perfectly fit the shape of the defect. Calcium phosphate was rapidly integrated into a newly formed bone network, just as we had expected.[31] Moreover, the self-setting properties of the superficial polymer contributed to maintain the granules in place into the defect.[17] This self-reticulating process is influenced by both the pH and the temperature; at physiological pH and temperature, this gelation process takes place in about 20 minutes.[24,25] Both the amount of CaP granules and the injected superficial polymer can be adapted perioperatively according to the specificity of the defect. Such a biphasic approach may provide an acellular ready-to-use and absorbable construct for osteochondral regeneration in a less invasive way than autologous transplants and without the requirement for a dedicated prosthetic implant.

This study has several limitations. The experimental design in sheep prevented the use of growing animals predisposed to OC. Adult sheep may not have the same bone healing modalities that growing large breed dogs have, and subsequent histological osteointegration features may not reflect the clinical situation. The number of animals was also limited, mainly for ethical reasons, but homogenous histological features were obtained in each tested condition. The absence of a negative control empty defect may also appear as a limitation. But both clinical experience and literature in animal and human patients have already shown that such large osteochondral defects may not heal spontaneously with a hyaline cartilage formation.[2-4,36,37] The major limitation remains that biphasic constructs were not evaluated in the same femoral condyle location as autografts and prosthetic implants. Cartilage and bone repair may be different between the axial intra trochlear site and the high load bearing area of the medial condyle, as has been reported in rabbits.[39] Results obtained from this original regenerative approach in donor sites of autologous transplants must therefore be considered as preliminary data, and biphasic constructs deserve additional study in femoral condyle defects.

In conclusion, biphasic constructs combining a self-setting chitosan/cellulosic superficial polymer and a CaP subchondral base led to hyaline cartilage and subchondral bone regeneration in donor sites of autologous transplants. This regenerative approach may eventually provide an alternative to autologous transplants or prosthetic implants for the treatment of OC dissecans lesions in animals.

ACKNOWLEDGMENTS

The authors thank Ronan Le Meur DVM and Juliette Petain DVM for surgical assistance during the experiment, and Gildas Rethore PhD and Joelle Veziers PhD for technical assistance.

CONFLICT OF INTEREST

The authors declare no financial or other conflicts of interest related to this study.

REFERENCES

1. Alford JW, Cole BJ. Cartilage restoration, part 1: basic science, historical perspective, patient evaluation, and treatment options. *Am J Sports Med.* 2005;33:295-306.
2. Cook JL, Hudson CC, Kuroki K. Autogenous osteochondral grafting for treatment of stifle osteochondrosis in dogs. *Vet Surg.* 2008;37:311-321.
3. Fitzpatrick N, Yeadon R, van Terheijden C, Smith TJ. Osteochondral autograft transfer for the treatment of osteochondritis dissecans of the medial femoral condyle in dogs. *Vet Comp Orthop Traumatol.* 2012;25:135-143.
4. Fitzpatrick N, Yeadon R, Smith TJ. Early clinical experience with osteochondral autograft transfer for treatment of osteochondritis dissecans of the medial humeral condyle in dogs. *Vet Surg.* 2009;38:246-260.
5. Fitzpatrick N, Van Terheijden C, Yeadon R, Smith J. Osteochondral autograft transfer for treatment of osteochondritis dissecans of the caudocentral humeral head in dogs: osteochondral autograft transfer for osteochondritis dissecans. *Vet Surg.* 2010;39:925-935.
6. Simonian PT, Sussmann PS, Wickiewicz TL, Paletta GA, Warren RF. Contact pressures at osteochondral donor sites in the knee. *Am J Sports Med.* 1998;26:491-494.
7. Reddy S, Pedowitz DI, Parekh SG, Sennett BJ, Okereke E. The morbidity associated with osteochondral harvest from asymptomatic knees for the treatment of osteochondral lesions of the talus. *Am J Sports Med.* 2006;35:80-85.
8. Cook J, Kuroki K, Bozynski C, Stoker A, Pfeiffer F, Cook C. Evaluation of synthetic osteochondral implants. *J Knee Surg.* 2013;27:295-302.
9. Husby KA, Reed SK, Wilson DA, et al. Evaluation of a permanent synthetic osteochondral implant in the equine medial femoral condyle. *Vet Surg.* 2016;45:364-373.
10. Egan P, Murphy S, Jovanovik J, Tucker R, Fitzpatrick N. Treatment of osteochondrosis dissecans of the canine stifle using synthetic osteochondral resurfacing. *Vet Comp Orthop Traumatol.* 2018;31:144-152.
11. Danielski A, Farrell M. Use of synthetic osteochondral implants to treat bilateral shoulder osteochondritis dissecans in a dog. *Vet Comp Orthop Traumatol.* 2018;31:385-389.
12. Bentley G, Biant LC, Carrington RWJ, et al. A prospective, randomised comparison of autologous chondrocyte implantation versus mosaicplasty for osteochondral defects in the knee. *J Bone Joint Surg.* 2003;85:223-230.
13. Hunziker EB, Lippuner K, Keel MJB, Shintani N. An educational review of cartilage repair: precepts and practice—myths and misconceptions—progress and prospects. *Osteoarthritis Cartilage.* 2015;23:334-350.
14. Horas U, Pelinkovic D, Herr G, Aigner T, Schnettler R. Autologous chondrocyte implantation and osteochondral cylinder transplantation in cartilage repair of the knee joint. *J Bone Joint Surg. Am.* 2003;85:185-192.
15. Knutsen G, Engebretsen L, Ludvigsen TC, et al. Autologous chondrocyte implantation compared with microfracture in the knee. *J Bone Joint Surg. Am.* 2004;86:455-464.
16. Kon E, Roffi A, Filardo G, Tesei G, Marcacci M. Scaffold-based cartilage treatments: with or without cells? A systematic review of preclinical and clinical evidence. *Arthroscopy.* 2015;31:767-775.
17. Flegeau K, Pace R, Gautier H, et al. Toward the development of biomimetic injectable and macroporous biohydrogels for regenerative medicine. *Adv Colloid Interface Sci.* 2017;247:589-609.
18. Di Martino A, Sittinger M, Risbud MV. Chitosan: A versatile biopolymer for orthopaedic tissue-engineering. *Biomaterials.* 2005;26:5983-5990.
19. Hao T, Wen N, Cao JK, et al. The support of matrix accumulation and the promotion of sheep articular cartilage defects repair in vivo by chitosan hydrogels. *Osteoarthritis Cartilage.* 2010;18:257-265.
20. Comblain F, Rocasalbas G, Gauthier S, Henrotin Y. Chitosan: a promising polymer for cartilage repair and viscosupplementation. *Biomed Mater Eng.* 2017;28:S209-S215.
21. Oprenyeszk F, Sanchez C, Dubuc JE, et al. Chitosan enriched three-dimensional matrix reduces inflammatory and catabolic mediators production by human chondrocytes. *PLoS One.* 2015;10(5):e0128362.
22. Shive MS, Stanish WD, McCormack R, et al. BST-CarGel treatment maintains cartilage repair superiority over microfracture at 5 years in a multicenter randomized controlled trial. *Cartilage.* 2015;6:62-72.
23. Merceron C, Portron S, Masson M, et al. Cartilage tissue engineering: from hydrogel to mesenchymal stem cells. *Biomed Mater Eng.* 2010;20:159-166.
24. Vinatier C, Gauthier O, Fatimi A, et al. An injectable cellulose-based hydrogel for the transfer of autologous nasal chondrocytes in articular cartilage defects. *Biotechnol Bioeng.* 2009;102:1259-1267.
25. Fatimi A, Tassin JF, Turczyn R, Axelos MA, Weiss P. Gelation studies of a cellulose-based biohydrogel: the influence of pH, temperature and sterilization. *Acta Biomater.* 2009;5:3423-3432.
26. Dhollander A, Sanchez V, Almqvist K, et al. The use of scaffolds in the treatment of osteochondral lesions in the knee: current concepts and future trends. *J Knee Surg.* 2012;25:179-186.
27. Kon E, Filardo G, Perdisa F, Venieri G, Marcacci M. Clinical results of multilayered biomaterials for osteochondral regeneration. *J Exp Orthop.* 2014;1:10.
28. Christensen BB, Foldager CB, Jensen J, Jensen NC, Lind M. Poor osteochondral repair by a biomimetic collagen scaffold: 1- to 3-year clinical and radiological follow-up. *Knee Surg Sports Traumatol Arthrosc.* 2016;24:2380-2387.
29. Berruto M, Delcogliano M, de Caro F, et al. Treatment of large knee osteochondral lesions with a biomimetic scaffold: results of a multicenter study of 49 patients at 2-year follow-up. *Am J Sports Med.* 2014;42:1607-1617.
30. Verhaegen J, Clockaerts S, Van Osch GJ, et al. TruFit plug for repair of osteochondral defects-where is the evidence? Systematic review of literature. *Cartilage.* 2015;6:12-19.

31. Bouler JM, Pilet P, Gauthier O, Verron E. Biphasic calcium phosphate ceramics for bone reconstruction: a review of biological response. *Acta Biomater*. 2017;53:1-12.
32. Bi L, Cheng W, Fan H, Pei G. Reconstruction of goat tibial defects using an injectable tricalcium phosphate/chitosan in combination with autologous platelet-rich plasma. *Biomaterials*. 2010;31:3201-3211.
33. Böttcher P, Zeissler M, Grevel V, Oechtering G, Maierl J. Mapping subchondral bone density of selected donor and recipient sites for autologous osteochondral transplantation in the canine stifle joint using computed tomographic osteoabsorptiometry: mapping subchondral bone density in the canine femur. *Vet Surg*. 2010;39:496-503.
34. Böttcher P, Zeissler M, Maierl J, Grevel V, Oechtering G. Mapping of split-line pattern and cartilage thickness of selected donor and recipient sites for autologous osteochondral transplantation in the canine stifle joint. *Vet Surg*. 2009;38:696-704.
35. Böttcher P, Zeissler M, Grevel V, Oechtering G. Computer simulation of the distal aspect of the femur for assessment of donor core size and surface curvature for autologous osteochondral transplantation in the canine stifle joint: surface curvature of the distal aspect of the femur. *Vet Surg*. 2010;39:371-379.
36. Iwasaki N, Kato H, Kamishima T, Suenaga N, Minami A. Donor site evaluation after autologous osteochondral mosaicplasty for cartilaginous lesions of the elbow joint. *Am J Sports Med*. 2007;35:2096-2100.
37. Burks RT. The use of a single osteochondral autograft plug in the treatment of a large osteochondral lesion in the femoral condyle: an experimental study in sheep. *Am J Sports Med*. 2006;34:247-255.
38. Kon E, Robinson D, Verdonk P, et al. A novel aragonite-based scaffold for osteochondral regeneration: early experience on human implants and technical developments. *Injury*. 2016;47 (Suppl 6):S27-S32.
39. Chen H, Chevrier A, Hoemann CD, et al. Bone marrow stimulation of the medial femoral condyle produces inferior cartilage and bone repair compared to the trochlea in a rabbit surgical model. *J Orthop Res*. 2013;31:1757-1764.

How to cite this article: Olive M, Boyer C, Lesoeur J, et al. Preliminary evaluation of an osteochondral autograft, a prosthetic implant, and a biphasic absorbable implant for osteochondral reconstruction in a sheep model. *Veterinary Surgery*. 2020;1–12. https://doi.org/10.1111/vsu.13373